THE HYDROGEN AND CHLORINE ISOTOPIC SIGNATURES OF HIGHLY SHOCKED EUCRITES. T. J. Barrett[1], A. Černok[2], G. Degli-Alessandrini[1], X. Zhao[1], M. Anand[1,3], I. A. Franchi[1] and J. Darling[4]. [1]School of Physical Sciences, The Open University, Walton Hall, Milton Keynes, MK7 6AA, UK (E-mail: thomas.barrett@open.ac.uk), [2]Centre for Applied Planetary Mineralogy, Department of Natural History, Royal Ontario Museum, Toronto, M5S 2C6, Canada [3]Department of Earth Sciences, Natural History Museum, London, SW7 5BD, UK, [4]School of Earth & Environmental Sciences, University of Portsmouth, Portsmouth, PO1 3QL, UK.

Introduction: Understanding the volatile inventory and isotopic compositions of meteorite samples is critical given the importance of these elements in a variety of cosmochemical and geochemical processes. As such there has been significant interest in their abundance and isotopic composition, particularly in the trace mineral apatite which is known to contain appreciable amounts of volatile elements [e.g. [1]. Since shock-induced deformation is pervasive to varying degrees throughout many meteorite samples, any variation in observed apatite crystal structure related to shock may affect their volatile composition.

Electron Backscatter Diffraction (EBSD) analyses provide crystallographic information at the µm and sub-µm length scales. In extraterrestrial samples, EBSD has mostly been used to interpret larger-scale plastic deformation [2] and shock deformation in geochronometers such as zircon and baddeleyite [e.g. 3-5]. Importantly, these studies highlight the significance of understanding deformation at the µm-scale when interpreting complex U-Pb data and the mobility of Pb. More recently, an increasing complexity in phosphate deformation features with shock pressure has been observed in extraterrestrial apatite and merrillite [6-8].

Preliminary work has previously been undertaken to investigate apatite microstructures in eucrites [9] and their link to volatile composition for samples with previously obtained volatile data [10]. In this study we conducted a targeted investigation of the H and Cl abundances and isotopic compositions of previously EBSD-mapped apatite grains in three eucrites with moderate to high shock grades. Data from this work will further explore the relationship between shock deformation and volatiles.

Samples: The three samples selected for this study are basaltic eucrites of shock grades ranging from moderate to highly shocked: Puerto Lápice (S3)[11], Cachari (S4), and Padvarninkai (S5)[12]. Bulk compositions of these samples are broadly similar to each other and other basaltic eucrites [11, 13]. Of these, only apatite in Cachari has been previously analyzed for Cl [14] and H [15].

Methods: The Cl content and isotopic compositions were measured using the Cameca NanoSIMS 50L at The Open University in scanning ion imaging mode using a modified protocol based on Stephant et al. [16], acquiring negative secondary ions of ^{12}C, ^{18}O, ^{35}Cl, ^{37}Cl, and $^{40}Ca^{19}F$ simultaneously on electron multipliers. Regions of interest (ROIs) were selected based primarily on the $^{35}Cl/^{18}O$ images.

Hydrogen analyses were conducted on top of the Cl isotope image pits using the same instrument in multi-collection mode based upon a well-established protocol [e.g. 17, 18] acquiring negative secondary ions of ^{1}H, ^{2}H, ^{13}C, and ^{18}O. Measured D/H ratios are spallation corrected.

Results: A total of 19 measurements from 12 individual apatite grains were collected for Cl and a total of 17 correlated H measurements were made on top of the Cl image pits (Fig. 1). Where possible within the same apatite grain, one measurement was taken where EBSD maps showed fewer deformation features and another measurement was taken where these maps indicated more complex microstructures to allow for intra-grain comparisons.

Apatite in the moderately shocked Puerto Lápice display a range in Cl content from ~ 750 to 1100 ppm with most analyses showing > 900 ppm Cl. Cachari and Padvarninkai contain more Cl overall, with Cl contents ranging from ~ 1000 to 1400 ppm.

The $\delta^{37}Cl$ values for apatite in Puerto Lápice (~ –3.4 ± 1.1 to −0.6 ± 1.1 ‰, 2σ) are within error of terrestrial values although typically lower (< −2 ‰). Both Cachari and Padvarninkai have relatively ^{37}Cl-enriched signatures (~ +5.4 ± 1.1 ‰ to ~ + 7.5 ± 1.2 ‰ and ~ + 3.0 ± 1.4 ‰ to ~ + 7.7 ± 0.9 ‰, respectively), similar to some previously analyzed basaltic eucrites [14][19], although Padvarninkai shows slightly more variability.

Water abundances for Puerto Lápice apatite grains exhibit a relatively large variation from ~ 240-840 ppm H_2O similar to the basaltic eucrite Millbillillie [17]. Cachari has a similar range to Puerto Lápice at ~ 186-780 ppm H_2O. Padvarninkai, on the other hand, has a relatively more restricted range in water content from ~ 965 to 1390 ppm H_2O, which is in keeping with other basaltic eucrites such as Stannern and Dar al Gani 844 [15, 17].

The hydrogen isotopic composition of Puerto Lápice ranges from δD ~ +90 ± 65 ‰ to +160 ± 58 ‰ (2σ) within error of many of the basaltic eucrites with similar H_2O abundance. The δD values for Cachari (~ −55 ± 135 ‰ to +98 ± 66 ‰) are within error of the

previous data point (−158 ± 24 ‰), however, apatite display a positive correlation between δD and H_2O content. Padvarninkai displays a similar range to Cachari (δD ~ −24 ± 70 ‰ to +129 ± 52 ‰) with the exception of a single data point that is lighter (~ −157 ± 55 ‰).

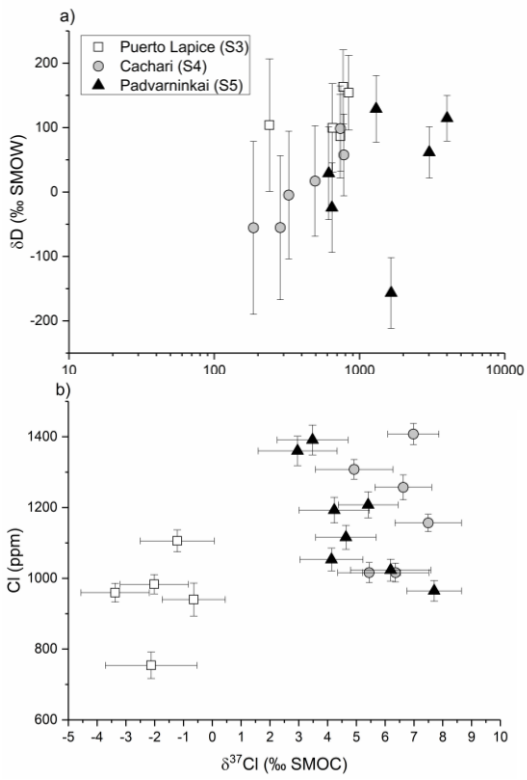

Figure 1: a) Plot of δD values versus H_2O content of analyzed samples. b) $\delta^{37}Cl$ values versus Cl content.

Discussion: Overall the abundance and isotopic composition of both H and Cl in these shocked basaltic eucrites are similar to the other (of lesser shock grades) basaltic eucrites, previously analyzed [14-15, 17, 19]. While the ROI analyses provide compositions comparable to that reported, the images reveal complex features that are visible at the sub-micron level. Given the small scale of these features the uncertainties associated with their $\delta^{37}Cl$ values are too large to reliably interpret any isotopic changes, however, the Cl content shows local variations (Fig. 2).

Other than a positive correlation between δD and H_2O content in Cachari (Fig. 1a) and a potential negative correlation between $\delta^{37}Cl$ and Cl content in Padvarninkai (Fig. 1b), there are no other obvious correlations within or between samples. Volatile abundance and isotopic composition are not obviously linked with deformation features revealed by EBSD, despite increasing shock grade. The consistent light Cl isotope composition observed in Puerto Lápice is interesting as only the unbrecciated Stannern trend eucrite North West Africa 5073 displays consistently similar values. These light $\delta^{37}Cl$ values (near –4 ‰) have been hypothesized to potentially record the primordial solar nebular signature.

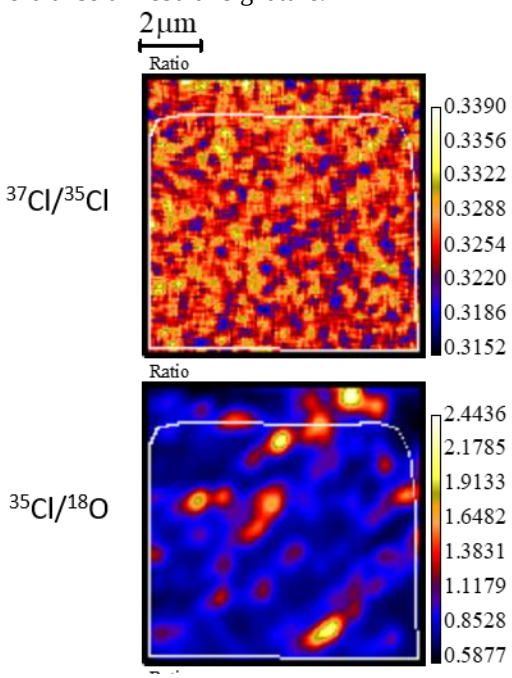

Figure 2: Isotope image displaying localized enrichments in Cl in a Cachari apatite grain. The ROI is outlined by white lines using L'IMAGE.

Conclusion: Data from this study highlight that whilst the microstructures observed in EBSD increase in complexity with shock grade [7][9], the abundance and isotopic composition of H and Cl in apatite within eucrites appears to remain unaltered.

References: [1] McCubbin F. & Barnes J. J *EPSL*, 526:115771. [2] Tkalcec B. J. & Brenker F. E. (2014) *MAPS*, 49:1202-1213. [3] Darling J. R. et al. (2016) *EPSL* 444:1-12. [4] White L. F. et al (2017) *Nat. Commun.*, 8:15597. [5] White L. F. et al (2018) *Geology*, 46:719-722. [6] Adcock C. T. et al. (2017) *Nat. Commun.*, 8:14667. [7] Černok A. et al. *MAPS*, 54:1262-1282. [8] Dyl K. A. et al. (2015) *LPSC XLVI*, Abstract #2927. [9] Barrett T. J. et al (2019) *LPSC L*, Abstract #1689. [10] Barrett T. J. et al (2018) *MetSoc LXXXI*, Abstract #6310. [11] Llorca J. et al. (2009) *MAPS*, 44:159-174. [12] Bischoff A. & Stöffler D. (1992) *Eur. J. Mineral.*, 4:707-755. [13] Mittlefehldt D. W. (2015) *Chem. Erde*, 75:155-183. [14] Sarafian A. R. et al. (2017) *EPSL*, 459:331-319. [15] Sarafian A. R. et al. (2014) *Science*, 346:623-626. [16] Stephant A. et al. (2019) *EPSL*, 523:115715. [17] Barrett T. J. et al. (2016) *MAPS*, 51:1110-1124. [18] Robinson K. L. et al (2016) *GCA*, 188:244-260 [19] Barrett T. J. et al *GCA*, 266: 582-597